

## EXPERIMENTAL IDENTIFICATION OF STIFFNESS AND ULTIMATE RESISTANCE OF BURIED SOIL-PIPE SYSTEMS

Adam CREWE<sup>1</sup>, Anastasios SEXTOS<sup>2</sup>, Rebecca STUBBS<sup>3</sup>, George MYLONAKIS<sup>4</sup>

### ABSTRACT

In context of pipeline design, the soil's stiffness and ultimate lateral resistance are critical values. Existing approximations for ultimate lateral resistance vary significantly and there are few expressions for the soil stiffness parameters. These parameters are implemented in soil constitutive models for pipeline design under different displacement induced conditions. This research focusses on the experimental investigation of the response of the soil-pipe system to enforced horizontal loading for application to natural gas pipelines. The study examines shallow burial depths ( $<5.5D$ ), using a section of solid acrylic pipe in dry Leighton Buzzard grade B sand. Plane-strain conditions have been replicated and experiments run to evaluate quantities for soil stiffness, through lab experiments and validated finite element analyses (FEA). Monotonic loading was applied onto the pipe within varied conditions, changing both burial depth and soil density to establish the relationship with soil stiffness. The FEA results were used to ratify such behaviors, establishing an analysis for displacement response and corresponding stiffness parameters. Absolute and relative stiffness values from both analyses were then compared with existing literature and the results reflect the importance of relative soil properties and expected displacements. Results find that horizontal loading within shallow burial depths induce 2D displacements, which could be modelled as vectors rather than horizontal displacements.

*Keywords: Soil stiffness; pipelines; soil-pipe interaction, experimental investigation*

### 1. INTRODUCTION

Soil stiffness influence the response of a soil-pipe system under earthquake-induced faulting, landslides, liquefaction, urban excavations and tunneling (O'Rourke, 1985). The exact failure displacement, ultimate force and failure mechanism are a product of in-situ stresses and soil parameters, therefore several expressions have been proposed in the literature and design documents. Relevant guidelines in the US (American Lifelines Alliance (ALA), 2005), consider some of these effects by mean of horizontal bearing capacity factors,  $N_{gh}$ , which are a function of peak friction angle,  $\phi'$  and burial depth,  $H$ . Commonly used Winkler soil models represent the soil stiffness via a series of parallel springs attached to the pipe. Each individual spring has stiffness constant value,  $K(x)$  based on hyperbolic functions for the force-displacement curves, which are simplifications of the soils non-linear behaviour as shown in eq. 1, where  $P$  is lateral force, and  $y$  is horizontal displacement.

Pipe-soil interaction is a complex phenomenon and modelling such interactions numerically is challenging, particularly given the extended geometry of the pipe, the associated subsoil conditions and the 2D or 3D site response under earthquake loading within the media crossed by the pipe. The resulting failure mechanisms due to lateral displacements are also not well defined due to multiple material and geometric nonlinearities near and on the soil-pipe interface, respectively. Previously numerical models have been validated through experimental results, and these simple equations, such as within ALA guidelines, have naturally stemmed from experimental literature. However, there are large discrepancies

---

<sup>1</sup> Associate professor, Department of Civil Engineering, University of Bristol, Bristol, UK

<sup>2</sup> Associate Professor, Department of Civil Engineering, University of Bristol, Bristol, UK & Aristotle University of Thessaloniki, Greece [a.sextos@bristol.ac.uk](mailto:a.sextos@bristol.ac.uk)

<sup>3</sup> Structural Engineer, at Mott MacDonald, UK

<sup>4</sup> Chair in Geotechnics and Soil-Structure Interaction, Department of Civil Engineering, University of Bristol, Bristol, UK & University of Patras, Greece

in existing literature due to different limitations and assumptions made within all experimental and analytical methodologies. For example, micro and macroscopic behaviour of soils is often not accounted for within analytical models (Roy, Hawlader, Kenny, & Moore, 2015) and this behaviour can govern failure mechanisms. The soil's stiffness value is a function of the interface conditions with the pipe, the soil's elastic modulus,  $E$ , Poisson's ratio,  $\nu$ , and the relative burial depth to diameter ratio,  $H/D$  (eq. 2). Stiffness can also be evaluated differently, depending on the soil's strain level, based on the non-linear nature of the soil behavior (Figure 1).

$$P = K(x).y \quad (1)$$

$$K(x) = \Gamma\left(\frac{H}{D}, \nu\right).E \quad (2)$$

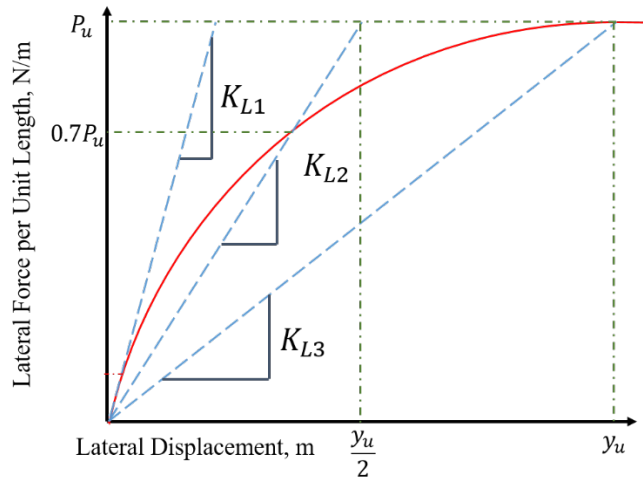


Figure 1: Lateral stiffness of the soil-pipe system (O'Rourke & Liu, 1999)

Table 1: Summary of the sand properties within existing experimental literature

<i>Sand density</i>	<i>Density, KN/m<sup>3</sup> (Ovesen, 1964)</i>	<i>Friction angle, ° (Ovesen, 1964)</i>	<i>Density KN/m<sup>3</sup> – Cornell Sand (Trautmann, 1985)</i>	<i>Friction angle, ° (Trautmann, 1985)</i>
Loose	16	30	14.8	31
Medium	17.3	35	16.4	36
Dense	18.7	40	17.7	44
Very Dense	20	45		

## 2. LATERAL P-Y CURVES WITHIN DESIGN CODES/STANDARDS

ALA defines the maximum lateral soil force per unit length,  $P_u$ , for sand as per equation 3, which incorporates a bearing capacity factor  $N_{qh}$  (Trautmann & O'Rourke, 1985). The equation for maximum horizontal elastic displacement,  $y_u$ , varies with density as shown by equation 4; yielding a range of values depending on burial depth, pipe diameter,  $D$  and coefficient  $A$  within equation 4. Interpretation of these equations is subjective as the density of such material tends to be relative based on the individual material properties, as seen within Table 1; however, no guidance is given to define the bounds. The values for upper and lower bounds (O'Rourke, 1999) are used in this study. Implementing these design charts as part of pipeline design therefore requires laboratory testing to find peak friction values for the material as well as accurate quantification of in-situ density.

$$P_u = \gamma H N_{qh} D \text{ (sand)} \quad (3)$$

$$y_u = (A)\left(H + \frac{D}{2}\right) \quad (4)$$

where  $A = 0.07 \sim 0.10$  for loose sand,  $0.03 \sim 0.05$  for medium sand, and  $0.02 \sim 0.03$  for dense conditions. Recent works (Kouretzis, Sheng, & Sloan, 2013) looked to create design charts for shallow burial ( $<5.5D$ ) backfilled trenches based on burial depth and relative density only, which would avoid this challenge within large scale applications where the backfill material may vary significantly over the length of a gas-pipeline. O'Rourke & Liu (1999) identify stiffness values depending on the corresponding strain level within the material, or so-called relative displacements. These stiffness expressions can be seen in Figure 1 and are based on the literature (Audibert & Nyman, 1977) considering initial tangential stiffness  $K_{L1}$ , secant stiffness at 70% of the ultimate lateral force,  $K_{L2}$ , and secant stiffness at ultimate lateral force,  $K_{L3}$ . Their values are shown below in equation 5. O'Rourke & Liu (1999) presented a bi-linearisation of the soil's behaviour with an expression for equivalent elastic soil spring constant as  $2P_u/y_u$ , which was adopted by ALA; in Figure 1 this corresponds to  $K_{L2}$  but depending on the shape of the force-displacement curve this is not always the case.

$$K_L = \alpha \frac{P_u}{y_u} \quad (5)$$

where  $\alpha = 6.67$  for  $K_{L1}$ ,  $\alpha = 2.7$  for  $K_{L2}$  and  $\alpha = 1$  for  $K_{L3}$ . To quantify and study the forces and displacements reported within the existing literature, values are herein normalised to the dimensionless force  $P/\gamma HD$ , where  $L$  is the length of the pipe and  $\gamma$  is the shear strain of the soil. Other important literature considered in this paper relates to experimental and analytical findings and the role played by plane-strain conditions, soil-pipe interaction, Mohr-Coulomb (MC) and Modified Mohr-Coulomb (MMC) modelling, and large scale testing. The influence of shear modulus,  $G$  and the elastic modulus  $E$  on soil behaviour has also been discussed. Overall, focus has been made on simulating behavioural trends with different burial depths and soil densities, within expected failure behaviours expressed qualitatively (Chaloulos, Bouckovalas, & Karamitros, 2017). Static stiffness values for axial springs have been proposed as a function of  $G$  (El Hmadi & O'Rourke, 1988), within the range  $1.0G < K < 3.0G$ , and updated within the range  $1.57G < K < 1.7G$  to account for small ground movement.

Other experimental studies have been conducted in the past to understand lateral pipeline-soil interaction in sand (Audibert & Nyman, 1977; Daiyan, Kenny, Phillips, & Popescu, 2011). Based on these experiments design curves for the bearing capacity factors have been concluded, predominantly from the work of (Trautmann & O'Rourke, 1983). Large scale experiments were also presented of dimensions 1.2m width x 2.3m length x 1.2m deep with the aim to measure the variation of maximum lateral soil force and the force-displacement as a function of pipe burial depth and soil density. Audibert's research looked at four diameters between 25.4mm and 254mm, O'Rourke with two pipe diameters, 102mm and 324mm. They looked at burial depths ranging from 1.5D to 11D and density from  $14.8 \text{KN/m}^3$  to  $17.7 \text{KN/m}^3$ . Tests reported to be working under plane strain conditions; their findings as well as others are summarized in Table 2 along with the results reported herein that will be discussed in the following section.

**Table 2: Expected displacements for ultimate lateral resistance of pipes in sand**

<i>Sand density</i>	<i>Trautmann &amp; O'Rourke (1985)</i>	<i>Audibert and Nymann (1977)</i>	<i>Das &amp; Seeley (1975)</i>	<i>Neely et Al. (1973)</i>	<i>This experiment (average values)</i>
Loose	0.13H	0.060H (D=25.4mm) 0.041H (D=61mm) 0.030H (D=114.3mm) 0.025H (D=254mm)	0.12H		0.11H (D=100mm)
Medium	0.08H			0.15H	
Dense	0.03H	0.036H (D=25.4mm) 0.026H (D=61mm) 0.022H (D=114.3mm) 0.019H (D=254mm)			0.06H (D=100mm)

Existing literature has limited experimental work that isolates parameters and their implications within the problem; due to the parametric nature of soil, specific graphs/equations can be difficult to maintain, and comparisons between works can be difficult, because density is not even a parameter that can directly be compared. Specifically looking at application to natural gas pipelines, where pipes are laid within very shallow, backfilled trenches (typically less than 2D burial depth) Chaloulos, 2017 found that critical parameters tend to govern the soil's response due to dilation and low stress conditions. However, ALA design codes begin their quantification of  $N_{qh}$  from a burial depth of 1.5D depending on the peak friction angle of the soil. This means that the design codes are quite inaccessible to researchers and designers, due to their reliance on density and peak friction angles. Making quantification of seismic risk to such pipelines challenging. Along these lines, this work aims to (a) design and execute experiments which isolate plane-strain behaviour whilst minimising boundary condition effects, (b) quantify experimental displacement responses for monotonic loading of a pipe-soil system, within a burial depth range of 1-5.25D and (c) study the failure mechanisms involved and their relationship with changing burial depth and density.

### **3. EXPERIMENT FOR LATERAL SAND STIFFNESS**

#### **3.1 *Scope of experiment***

Given that the emphasis of this study is on natural gas pipelines, which typically sit within backfilled shallow trenches, burial depth is limited to 5.25D (Chaloulos, 2017); most previous literature for pipeline behaviour extends beyond this range, however, this would have significantly increased scale of experiment with minimal benefit. An experimental procedure was developed and tested that created a repeatable set of test conditions where both the burial depth and sand density could be varied to acquire lateral force-displacement curves. Experimental dimensions were chosen so that ultimate lateral force could be reached within the range of the apparatus for all burial conditions specified enabling a full range of stiffness values;  $K_{L1}$ ,  $K_{L2}$ , and  $K_{L3}$  to be evaluated. Scale effects of the experiment are likely, due to the reduction of geo-static stresses, therefore ideally the material should be a looser density than experienced in real terms to represent this, and better mimic the critical state behaviour.

#### **3.2 *Experiment scale and dimensions***

To decide on scale and dimensions of the experiment, existing literature was reviewed to establish the expected influence of boundary conditions, and these findings informed experimental dimensions. The width of the box is dictated by three factors: the influence of friction between the sand and the near tank surfaces, achieving plane strain conditions, and the achievable practical width for experimental preparation. The length and depth of the tank is dictated by the influence of distant lateral boundaries, as well as burial depths required. According to the literature (Matsii & Derevenets, 2005) for piles being tested for lateral displacements, the minimum spacing to avoid interaction was 2D-4D, where  $D$  is pile diameter. In other studies (Yimsiri, Soga, Yoshizaki, Dasari, & O'Rourke, 2004) a minimum distance to the boundary was estimated as 6D. Similarly, (Drescher, Vardoulakis, & Han, 1990) used soil samples of 40mm width to acquire data for bi-axial testing of soils under plane-strain conditions; the influence of friction with the lateral boundary plates on plane strain testing caused artificial increased soil strength, and therefore width was increased to 2/3D to reduce the stiffening effects on the results. Practitioners found that the optimum results for analytical testing were for width  $< D/10$ ; this yielded the best failure mechanisms within a 2D plane; on the contrary, thickness' greater than this found that failure mechanisms tended to angle into 3D planes within the body.

In conclusion, the tank had to be wide enough that a consistent soil sample can be prepared, secured and tested appropriately; a very thin tank would cause potential inaccuracies due to friction with boundary conditions and a wide one would yield far higher results for ultimate failure load due to volume of resisting material, causing more sophisticated equipment to be needed. Based on the above consideration, the tank dimensions have been specified as 0.1m wide x 1.6m long x 1.1m deep, with a pipe diameter of 100mm giving the tank thickness of 1D (Figure 2). Isolation of plane-strain conditions and preparation of the sand is practically possible to achieve within this width whilst reducing effects of friction, arching of the sand and minimising 3D failure mechanisms. The length of the tank is

apparently a compromise, based on creating asymmetry that allows multi-functionality of the tank with multiple orientations. The pipe location is  $5.5D$  from the surrounding edges, giving a minimum distance of  $4.55D$  when at maximum displacement; within this research, monotonic loading, from left to right, into the larger volume of sand was undertaken with the aim to keep stiffness influence from lateral boundaries to the minimum.

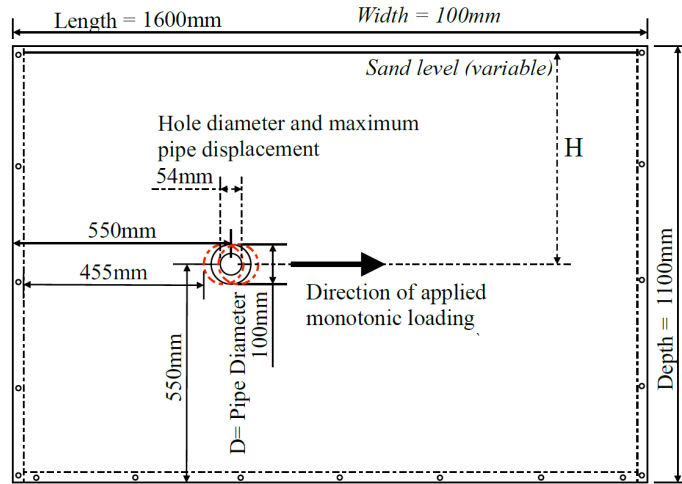


Figure 2: Tank elevation dimensions, all references to the tank dimensions and displacements are in respect to this orientation.

### 3.3 Experiment apparatus

The experimental set up includes a narrow Perspex tank made of 5 sheets of 25mm transparent Perspex, with the top side left open for compaction and ease of restraining tank. A large restraint frame clamped to the floor and to the tank directly restrained any movement and isolated transfer of forces straight from the pipe to the surrounding soil. Due to focus on system behaviour not pipe specifically, a solid acrylic pipe was used rather than a hollow cylinder like traditional pipe, for simplicity; it was cut to 100mm diameter and 99mm width with two O-rings that sat on its circumference to create an interface with the Perspex sheets with minimal friction. Also, a series of instrumentation, including three celescopes and a load cell was integrated into the tank. Load application was via a hand actuator transferring forces to the pipe via a simple mechanism to flat nylon ropes attached to a threaded bar into the pipe. The ropes were very light in weight and critically has very low resistance to bending that did not add residual forces to the system as seen in Figure 3. This setup was preferable to pushing the pipe into an active zone of soil, due to long arms needed to transfer force between the actuator and the pipe, which would have been prone to buckling. Restraining or supporting these arms would potentially impact the transferred forces, the displacement direction or the corresponding failure mechanism.

As series of calibrations were made quantitatively and qualitatively within this set up, in order to evaluate the residual forces present and the impact of adjustments to the system. Quantitative calibrations of all celescopes and load cell were undertaken, with repeat readings used, to gain calibration factors that were applied to the experimental data. During these calibrations, it was found the horizontal and vertical celescopes added antisymmetric loading due to their resistances onto one side of the pipe, causing it to no longer sit flush to the inside of the Perspex sheets. Therefore, to remove the influence of these residual forces an additional celesco was added at an opposing angle to the resultant force of the others (Figure 3).



Figure 3: Photographs of experimental setup, during filling of a preliminary loose experiment (left) the load transfer mechanism with load cell (right).

To stiffen the tank steel bars were added horizontally below the pipe to prevent obstruction of failure surfaces and to avoid interference with the load application. This was necessary due to deflections of the Perspex sheets with self-weight of the sand; the Perspex appeared to be less stiff than initially calculated and meant that the tight tolerances between the pipe, O-rings and the sheets were exceeded. During loading and displacement of the pipe, this deflection allowed sand grains to move around the O-rings and through the holes in the tank walls. In some cases, this loss was minimal but in other cases was relatively significant. To accommodate this additional foam washers were added between the pipe and the O-rings to give extra elasticity to the seal, and close the gap caused by such deflection – of approximately 1mm per sheet. Although these bars reduced the effects of deflection under self-weight, under large load applications such as within the deeper burial depths, the sheets appeared to deflect locally under large transverse forces, causing sand to again move into any gaps opening within the seal.

### 3.4 *Limitations of the experimental methodology within this research*

Within this experimental setup there are several aspects that were not considered, namely: (a) application to partially saturated or saturated conditions, although it may be possible if the apparatus is adapted (b) application to very deep burial depths of the pipe, ( $>5.25D$ ); (c) materials with cohesion – the impact of friction with the boundaries would be much more significant; (d) cyclic loading, although the actuator system could be adapted in order to achieve this; (e) displacement of pipe beyond  $0.54D$ , into the realm of very large displacements and extensive residual forces; (f) different interface condition frictions; (g) pipe deformations or strains induced in the pipe itself; (h) measurement of soil pressures on the pipe's surface; (i) impact of pipe's self-weight in results; (j) direct impacts of scale effects due to reduction of effective stresses around the soil, affecting the material's elastic and shear modulus properties.

### 3.5 *Test procedure*

The main steps of the testing procedure are summarized in the following. A list of the experiments undertaken is provided in Table 2.

1. Define burial depth required and set up horizontal marker on outside of tank for reference.
2. Fill tank in intervals of 50mm, pouring approximately 8kg of sand at a time uniformly across the top, to create consistent density across the tank's length.
3. Flatten and compact each layer if necessary (medium and dense tests) via the use of a timber baton and a poker vibrator onto the soil's surface, in increments along the tank's length, avoiding touching the Perspex sheets.
4. Before adding the pipe, fill and compact to a level 2.5cm below the bottom of the hole so that the pipe sits at mid-depth within it; place pipe onto soil layer with bolt holes approximately 2mm from the left-hand side of the hole in the Perspex, so that the pipe's displacement is

- maximized. Support pipe whilst screwing threaded bar into both sides.
5. Fill tank carefully around the pipe's lower half, ensuring full backfill under its lower side. Compact sand at the pipe's mid depth and repeat at 1cm above its surface. Continue filling the tank evenly in 50mm layers until desired burial depth is obtained, ensure a level surface and regular density throughout.
  6. Attach loading straps and instrumentation to the pipe, apply small amount force to the straps via the hand actuator so that the catenary is taken up.
  7. Start acquisition system and video recording, slowly apply force via the hand actuator until the pipe reaches close to the hole's edge on the right-hand side.
  8. Unload and stop acquisition, reset for next experiment.

Table 3: List of experiments undertaken, firstly loose and then a series of denser experiments.

<i>Experiment</i>	<i>Repeats</i>	<i>Sand density (KN/m<sup>3</sup>)</i>	<i>Burial depth (mm)</i>	<i>Experiment</i>	<i>Repeats</i>	<i>Sand density (KN/m<sup>3</sup>)</i>	<i>Burial depth (mm)</i>
Test 1	3	14.6	150	Test 11	1	15.4	150
Test 2	1	14.6	135	Test 12	1	15.4	250
Test 3	3	14.6	130	Test 13	2	15.4	350
Test 4	3	14.6	100	Test 14	3	15.4	450
Test 5	4	14.6	525	Test 15	2	15.4	525
Test 6	2	14.6	250				
Test 7	3	14.6	350				
Test 8	2	14.6	450				

NOTE: The densities achieved were  $\pm 0.1\text{KN/m}^3$  for the medium-dense state and  $\pm 0.3\text{KN/m}^3$  for the loose.

### 3.6 Compaction testing of sand

To densify the sand, various forms of vibration were considered and the impact on the density was evaluated. Leighton Buzzard sand is relatively coarse and poorly graded, therefore was not very sensitive to compaction methods; during preliminary compaction testing of the sand using very thin layers made a small amount of difference within density observed, Table 3.

Table 4: Summary of compaction of sand tests, using approximately 9kg of sand

<i>Test</i>	<i>Layer depth (cm)</i>	<i>Density (KN/m<sup>3</sup>)</i>	<i>Test</i>	<i>Layer depth (cm)</i>	<i>Density (KN/m<sup>3</sup>)</i>
1	15	16.2	3	5	16.6
2	3	16.7	4	Natural condition	15.9

As can be seen, the density achieved in the experiments was less than expected, this appears to be due to its grading and the pluviation that occurs when pouring the sand into the tank. Due to the volume of material, small vertical and horizontal stresses and small disturbance within the tank it does not naturally consolidate and retains this loosened state.

## 4. EXPERIMENTAL RESULTS

### 4.1 Force-vs displacement relationship with ranging burial depths

Presented within Figure 4 and Figure 5 are the displacement responses to applied lateral force, normalised for comparative means. Loose sand showed no peak in the force-displacement curve; the peak value was equal to the residual. For less than 3.5D burial depth maximum force was reached, however, for the deeper burial depths there was no plateau within the data. The so-called medium-dense responses showed peak behaviour, and therefore both peak and residual forces are expressed within

Table 4. There is some uncertainty within all the values summarised within Table 4 due to the difficulty in defining the point of failure and therefore these ultimate values, cases where this is prevalent are shown by the “+” indicator within **Error! Reference source not found.** Where the maximum force value was not reached, and the maximum value observed was taken as this, shown by the “\*” indicator.

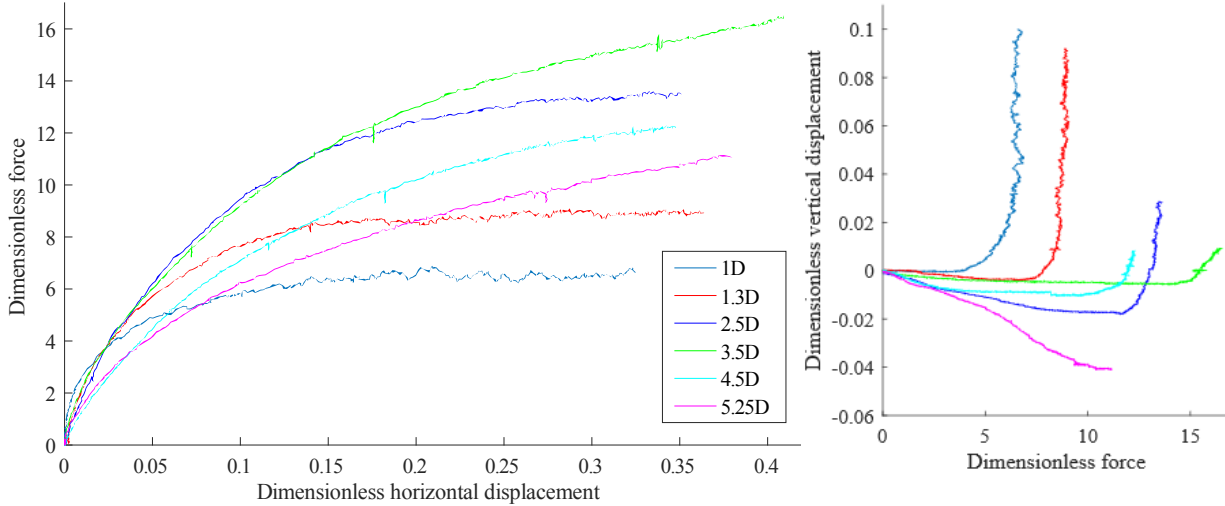


Figure 4: Force - displacement curve for loose sand. Force-horizontal displacement (left), vertical displacement-force (right).

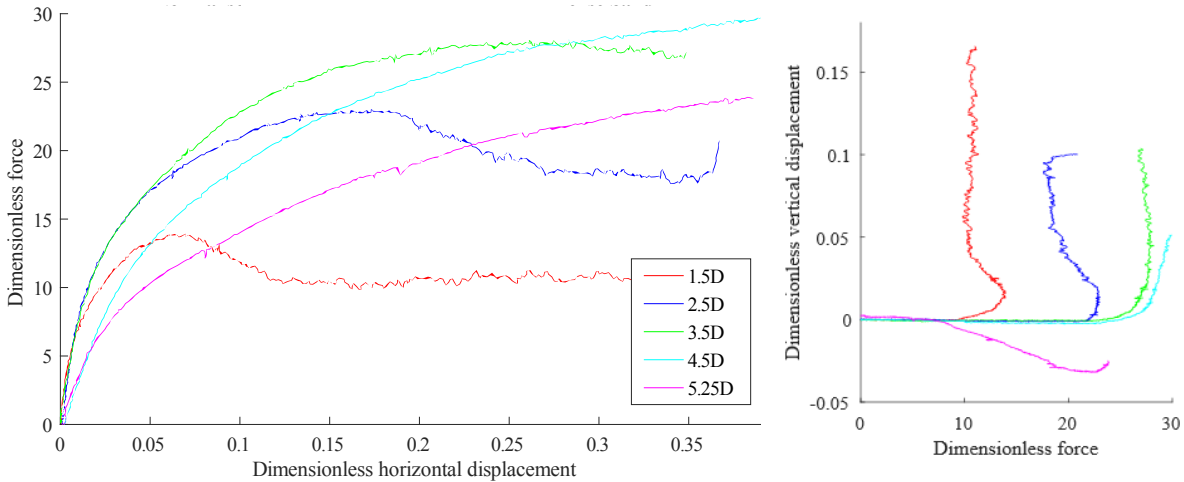


Figure 5: Force-displacement responses for dense sand. Force-horizontal displacement (left), vertical displacement-force (right).

In all experiments an initial force was needed to begin displacement of the sand, above that of the residual forces within the experiment. This initial force was not consistent but generally appeared to increase with burial depth. If related to friction either within the material or in relation to boundary conditions this would increase due to increased normal stresses to the surface near to the pipe. Inclusion or exclusion of this value in the results makes a significant difference as this initial force varies between 8-32% of the maximum force observed, with the most influenced values being at low burial depths. Observed forces are higher than expected due to potential impacts of trapped sand between the pipe and the tank walls, friction with the tank walls, and friction within the load application. Analysis of the residual forces within the experiment indicated that they appeared to be quite random, however with increasing number of tests, and more robust and consistent techniques, 19.3N was found to be the consistent value for step 6 of the experimental procedure. No adjustments were taken for friction with the boundary conditions due to the unknown quantification of their interaction. During testing sand often propagated and became trapped within the O-ring seals, and once this occurred forced open a larger gap

for more to move into; this meant that the pipe could become relatively stuck as its displacement was extended, and allowed sand to escape. It is considered that these sand losses would have had negligible effects on the forces exerted but the trapping of sand and consequentially increased friction would have significantly affected results at higher values of displacement, explaining why a plateau of maximum force was not seen in the results of several experiments.

The right chart of Figure 4 and Figure 5 shows how the vertical displacement varies with applied load, plotted with opposite axis for ease. This shows the magnitude of such displacements between the experiments and where within the load application they present; the majority of the movement is beyond 70% of the ultimate force. The magnitude of the displacement is largest within the shallow burial depths, indicating stronger dilation effects. The downward direction seen within some of the deeper burial conditions is considered to be due to the pipe’s initial positioning within the hole or consolidation under the pipe with loading. Due to the fixed location of the actuator, vertical displacements relative to the centreline of the apparatus mean that a small component of the applied force act against such displacements, however within the range of the experiment the magnitude of this force is minimal.

Table 5: Comparison of experimental results and theoretical values for ultimate and residual force with corresponding displacement

$\gamma_d = 14.6 \text{KN/m}^3$		<i>Experimental</i>		<i>Theoretical</i>		
Burial Depth H/D	$y_u$ (mm)	$P_{ultimate}$ (N/m)	$y_u$ lower limit (mm)	$y_u$ upper limit (mm)	$P_{ultimate}$ (N/m)	
1	13.7	970	10.5	15.0	725	
1.3	17.6	1612	12.6	18.0	943	
2.5	32.6*	5092*	21.0	30.0	2211	
3.5	39.7*	8201*	28.0	40.0	3756	
4.5	38.1*	9162*	35.0	50.0	5388	
5.25	38.5*	9168*	40.3	57.5	6242	

$\gamma_d = 15.4 \text{KN/m}^3$		<i>Experimental</i>			<i>Theoretical</i>	
Burial Depth H/D	$y_u$ (mm)	$P_{ultimate}$ (N/m)	$P_{residual}$ (N/m)	$y_u$ lower limit (mm)	$y_u$ upper limit (mm)	$P_{ultimate}$ (N/m)
1.5	6.4	3192	2377	6.0	10.0	1566
2.5	17.3	8795	7088+	9.0	15.0	3032
3.5	26.2*	15160*	14510*	12.0	20.0	4835
4.5	26.4*	19092*	N/A	15.0	25.0	7184
5.25	38.6*	19180*	N/A	17.3	28.8	8865

NOTE: +Value taken where readings began to fluctuate. \*Value taken as maximum observed within experiment

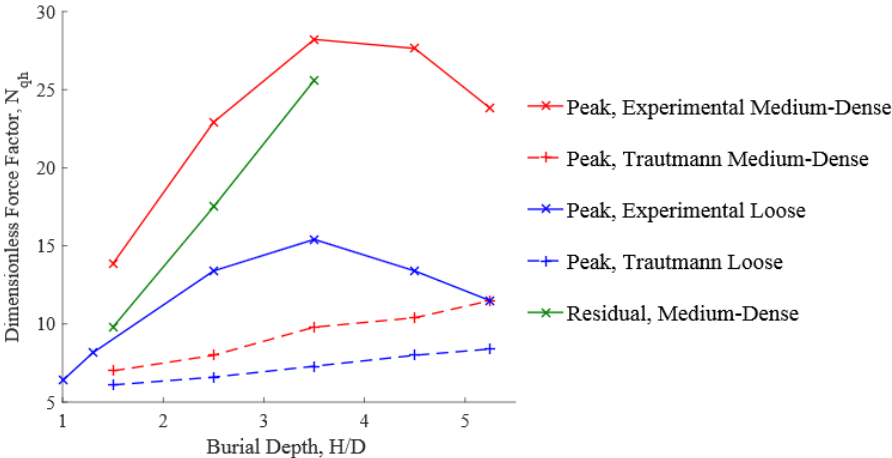


Figure 6: Dimensionless force factors for experimental data

Error! Reference source not found. demonstrates that the ultimate displacement for the low burial

depths fits well within the existing predictions, however the ultimate force has increased significantly, generally by a factor of 2. Figure 4 and Figure 5 show that the ultimate force does not appear to have been reached beyond 3.5D as the dimensionless force factor peaks at this value; within Figure  $N_{qh}$  expected values are also plotted for comparison purposes from ALA guidelines using experimental parameters. Figure 5 illustrates that within the medium-dense state, the maximum value of force reduces relative to the residual value with depth; this reduction of peak behaviour could be contributed to by the increasing frictional forces acting against the displacement and needs to be confirmed with more testing. **Error! Reference source not found.** also illustrates that the ultimate displacements generally agree with the findings of Trautmann, and O'Rourke (1985) and again indicate that the medium-dense condition is so despite the low density.

**5. INFLUENCE OF FAILURE MECHANISM**

Within the shallow burial depths an active wedge develops in front of the pipe with a shallow angle, and a passive wedge with steeper angle behind, as shown in Figure 7, consistent with Rankine theory. The sand's surface illustrates such behaviour of large dilation in front of the pipe and a loss of material behind. However, within deeper burial depths, smaller, more circular failure mechanisms are observed, starting in front of the pipe leading to the back-top face, which mobilise less sand than the shallower mechanism, resulting in less dilation of sand in front of the pipe, and less movement observed on the surface. The secondary shear plane still develops behind the pipe, and connects to the surface, allowing sand to flow down behind the pipe via passive behaviour to fill any voids created. A hole under the pipe forms in most cases, where the sand cannot act to completely backfill the voids, especially where movement is upward as well as horizontal as per shallow burial depths.

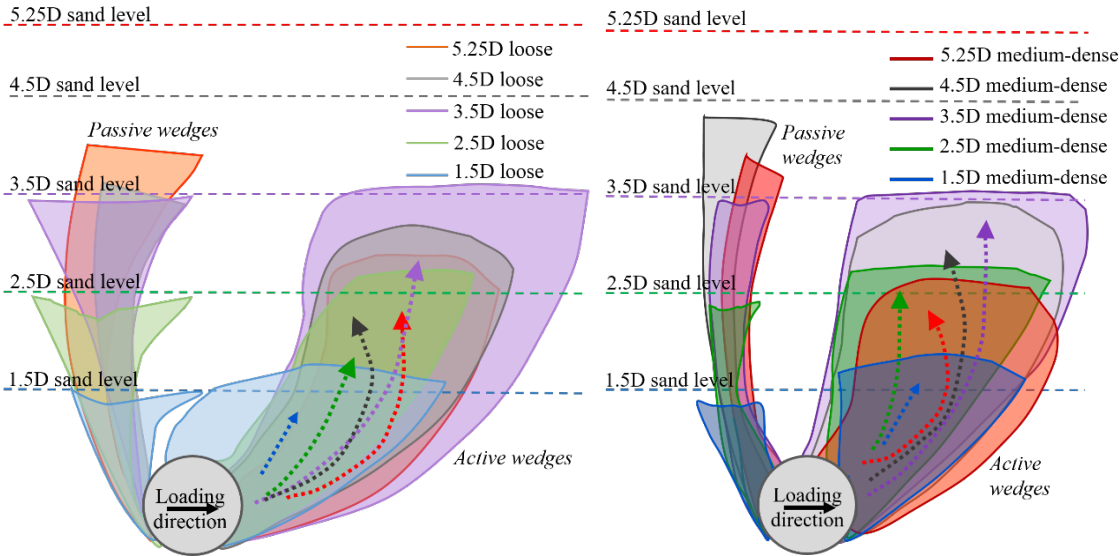


Figure 7: Comparison of failure mechanisms between different burial depths (a) loose (b) medium dense

Figure 8 also shows the differences between the failure surfaces and therefore the corresponding mobilised soil wedges between the different burial depths and soil densities, the shaded areas move due to either active (right-hand-side of pipe) or passive conditions (left-hand side), the arrows give a general direction to this movement. Within the dense condition, the friction angles also increase and enables steeper wedge angles comparatively, a larger area of soil behind the pipe within loose experiments enables larger changes of height of the soil at the surface in this region, particularly at low burial depths. With increasing burial depths the shape of the failure surface is modified due to higher confining pressures and increased friction angles; increasingly becoming more curved, disconnecting from the soil surface after burial of 3.5D. The size of this mobilised area of soil reduces significantly greater than 3.5D, which may contribute to why 3.5D appears to have higher than expected forces. The behaviour

seen here reinforces findings within Chaloulos et al. (2017), for general shear failure, type 1, and local shear failure, type 3 and the intermediate shear failure, type 2.

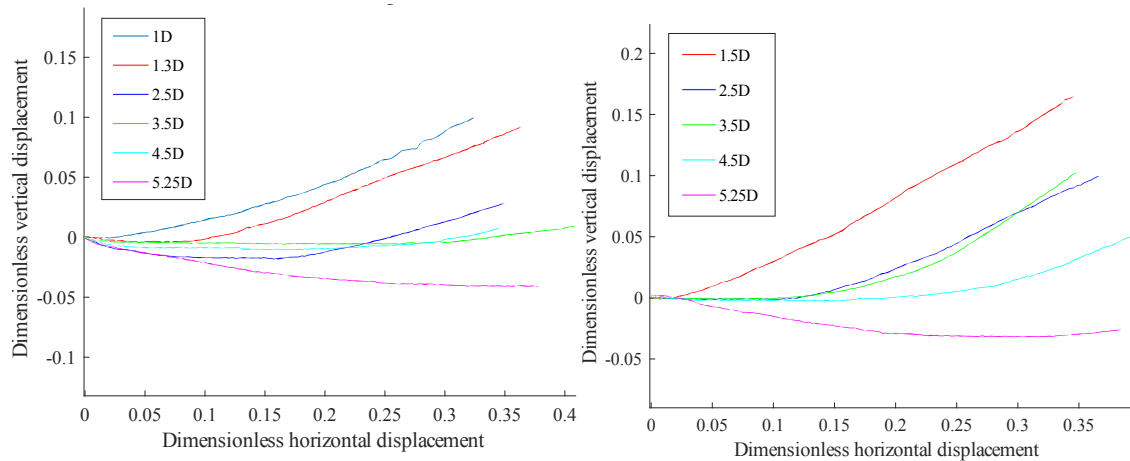


Figure 8: Displacement trajectories for loose (left) and dense sand (right).

## 5. CONCLUSIONS

This paper describes an experimental study of soil-pipe interaction, particularly of the displacement responses to laterally applied loading for the case of coarse grained sand under plane strain conditions. Emphasis is placed on burial depths between 1-5.25D with the aim to investigate stiffness and ultimate resistance implications for natural gas pipelines. A literature review shows the extent of current work in experimental and numerical fields; however, few focus their efforts on quantifying soil stiffness parameters in relation to implementation in modelling software.

Test results indicate that the experimental apparatus as a preliminary design are well founded, however work needs to be done to quantify frictional interfaces as this appears to be significant within the results, because of their relative magnitudes particularly at low burial depths. The displacement responses are favorably comparable to other experimental results and the general trends of the data indicate that the sand used does respond similarly to loose and then medium-dense conditions despite its density being approximately  $1\text{KN/m}^3$  less than anticipated, this highlights the subjective nature of interpreting the design codes and the geotechnical understanding necessary of the design conditions.

As part of this research, maximum forces encountered in the experimental analysis were approximately 2x higher and this is thought to be due to sand grains jamming the seal between the pipe and tank sides. This is very prominent within Leighton Buzzard sand due to its coarse nature, which would significantly increase the friction between the pipe and the Perspex sheets. Repeating such tests with sands of different geotechnical properties would help quantify such impacts on results.

In particular, the dimensionless curves are dominated by the 3.5D burial depth in both loose and medium-dense conditions. This is thought to be related to the relative size of the failure wedge being mobilised, as the 3.5D wedge is the largest due to transitioning to more circular failure mechanism shape at deeper depths. This force increase is amplified if friction with the Perspex tank sides is significant. Due to these frictional effects, residual forces were not reached in some of the deeper burial conditions contrary to expectations. The displacement measurements recorded within this research indicate 2D movements of the pipe as a response to lateral forces, therefore conventional horizontal force-displacement curves only capture one dimension of the resultant response. It is proposed that 2D coupled springs are used to describe such soil-pipe system responses analytically, which capture the vector displacements. The magnitude of vertical displacement increases significantly post 70% of the maximum force, especially once residual forces have been reached; in combination to their low values for ultimate displacement, this means that for very shallow pipelines subjected to large displacements, shallow pipes are more vulnerable of moving to the surface. This directly impacts seismic vulnerability and other causes of PGDs. Further research is currently undertaken that involves repetition of the tests for different tank widths, refined numerical verification and explicit consideration of friction effects between the soil and the tank surfaces.

## 6. ACKNOWLEDGMENTS

This work was supported by the Horizon 2020 MSCA-RISE-2015 project No. 691213 entitled "Experimental Computational Hybrid Assessment of Natural Gas Pipelines Exposed to Seismic Risk (EXCHANGE-RISK)". This support is gratefully acknowledged.

## 7. REFERENCES

- American Lifelines Alliance (ALA). (2005). *Guidelines for the Design of Buried Steel Pipe* (Vol. 2001).
- Audibert, J. M. E., & Nyman, K. J. (1977). Soil restraint against horizontal motion of pipes. *Journal of the Geotechnical Engineering Division, ASCE*, 103(GT10), 1119–1142.
- Chaloulos, Y. K., Bouckovalas, G. D., & Karamitros, D. K. (2017). Trench effects on lateral p-y relations for pipelines embedded in stiff soils and rocks. *Computers and Geotechnics*, 83, 52–63. <https://doi.org/10.1016/j.compgeo.2016.10.018>
- Daiyan, N., Kenny, S., Phillips, R., & Popescu, R. (2011). Investigating pipeline–soil interaction under axial–lateral relative movements in sand. *Canadian Geotechnical Journal*, 48(11), 1683–1695.
- Drescher, A., Vardoulakis, I., & Han, C. (1990). A biaxial apparatus for testing soils. *Geotechnical Testing Journal*, 13(3), 226–234.
- El Hmadi, K., & O'Rourke, M. J. (1988). Soil Springs for Buried Pipeline Axial Motion. *Journal of Geotechnical Engineering*, 114(11), 1335–1339.
- Kouretzis, G. P., Sheng, D., & Sloan, S. W. (2013). Sand-pipeline-trench lateral interaction effects for shallow buried pipelines. *Computers and Geotechnics*, 54, 53–59. <https://doi.org/10.1016/j.compgeo.2013.05.008>
- Matsii, S. I., & Derevenets, F. N. (2005). Application of finite-element method to investigate interaction between slide-prone soils and piles. *Soil Mechanics and Foundation Engineering*, 42(4), 120–126.
- O'Rourke, M. J., & Liu, X. (1999). *Response of Buried Pipelines Subject to Earthquake Effects, Monograph Series #3. Multidisciplinary Center for Earthquake Engineering Research, University at Buffalo.*
- Roy, K., Hawlader, B., Kenny, S., & Moore, I. (2015). Finite element modeling of lateral pipeline–soil interactions in dense sand. *Canadian Geotechnical Journal*, 53(3), 490–504.
- Trautmann, C. H., & O'Rourke, T. D. (1983). *Behaviour of pipe in dry sand under lateral and uplift loading, Geotechnical Engineering Report 83, School Civil and Environmental Engineering, Cornell University.*
- Trautmann, C. H., & O'Rourke, T. D. (1985). Lateral force-displacement of buried pipe response. *Journal of Geotechnical Engineering*, 111(9), 1077–1092. [https://doi.org/0733-9410/85/0009-1077/\\$01.00](https://doi.org/0733-9410/85/0009-1077/$01.00)
- Yimsiri, S., Soga, K., Yoshizaki, K., Dasari, G. R., & O'Rourke, T. D. (2004). Lateral and upward soil-pipeline interactions in sand for deep embedment conditions. *Journal of Geotechnical and Geoenvironmental Engineering, ASCE*, 130(8), 830–842.